Antiproton to proton ratios in Au+Au collisions at $\sqrt{s_{NN}} = 130$ GeV as function of rapidity and centrality

I. G. Bearden[8], D. Beavis[1], Y. Blyakhman[7], J. Brzychczyk[4], B. Budick[7], H. Bøggild[8], C. Chasman[1], C. H. Christensen[8], P. Christiansen[8], J. Cibor[5], R. Debbe[1], J. J. Gaardhøje[8], K. Grotowski[4], K. Hagel[9], O. Hansen[8], A. Holm[8], A. K. Holme[2], H. Ito[1], E. Jakobsen[8], A. Jipa[11], J. I. Jordre[10], F. Jundt[3], C. E. Jørgensen[8], T. Keutgen[4], E. J. Kim[6], T. Kosic[4], T. M. Larsen[2], J. H. Lee[1], Y. K. Lee[6], G. Løvhøiden[2], Z. Majka[4], A. Makeev[9], B. McBreen[1], M. Murray[9], J. Natowitz[9], B. S. Nielsen[8], K. Olchanski[1], J. Olness[1], D. Ouerdane[8], R. Płaneta[4], F. Rami[3], D. Roehrich[10], B. Samset[2], S. Sanders[12], R. A. Sheetz[1], Z. Sosin[4], P. Staszel[8], T. F. Thorsteinsen[10+], T. S. Tveter[2], F. Videbæk[1], R. Wada[9], A. Wieloch[4], and I. S. Zgura[11]
The BRAHMS Collaboration

[1] Brookhaven National Laboratory, Upton, USA
[2] Fysisk Institutt, University of Oslo, Blindern, Norway
[3] IReS, University Louis Pasteur, Strasbourg, France
[4] Jagiellonian University, Krakow, Poland
[5] Institute of Nuclear Physics, Krakow, Poland
[6] Johns Hopkins University, Baltimore, USA
[7] New York University, New York, USA
[8] Niels Bohr Institute, University of Copenhagen,Denmark
[9] Texas A&M University, College Station, USA
[10] University of Bergen, Norway
[11] University of Bucharest, Romania
[12] University of Kansas, USA
[+] *Deceased*

Version: ppbardraft.2.31.tex,April 2, 2001

Abstract

Measurements with the BRAHMS detector of the antiproton to proton ratio at central ($y \approx 0$ and $y \approx 0.7$) and forward ($y \approx 2$) rapidities for three different collision centralities, for Au+Au reactions at $\sqrt{s_{NN}} = 130$ GeV are presented. For collisions in the centrality range $(0-40\%)$ $N(\bar{p})/N(p) = 0.62 \pm 0.06$

at $y \approx 0$, 0.59 ± 0.05 at $y \approx 0.7$ and 0.44 ± 0.04 at $y \approx 2$. The ratios are found to be nearly independent of collision centrality and transverse momentum. The $N(\pi^-)/N(\pi^+)$ ratio has been determined to be near unity for three rapiditiy values ($y \approx 0, 1$ and 3). The measurements demonstrate that the antiproton and proton rapidity densities vary differently with rapidity, and indicate that a net-baryon free midrapidity plateau (Bjorken-limit) is not reached at this RHIC energy.

PACS numbers: 25.75.-q; ....

The reaction mechanism between heavy ions at high energies is expected to evolve from full stopping to complete transparency with increasing collision energy. In the case of full stopping, the baryons of the colliding nuclei will be be shifted from the rapidity of the incident beam to midrapidity ($y \approx 0$), leading to the formation of a central zone with significant net-baryon density. In the case of full transparency, also called the Bjorken limit [1], the baryons from the interacting nuclei will, after the collision, also be shifted from beam rapidity, but mid-rapidity will be devoid of original baryons. In this region, the net-baryon density is zero, but the energy density is high. Almost complete stopping is observed for Au+Au reactions at AGS energies ($\sqrt{s_{NN}} \approx 5$ GeV). In reactions between lead nuclei at SPS energies, $\sqrt{s_{NN}} = 17$ GeV, transparency begins to set in, and systematics suggest that maximum baryon density occurs at energies intermediate between AGS and SPS (see e.g. [2, 3]). The situations of maximum baryon density and of vanishing net-baryon density at midrapidity give rise to entirely different initial conditions for the possible creation of a deconfined quark-gluon system.

The rapidity dependence of the antiproton to proton ratio in collisions between Au nuclei at the Relativistic Heavy Ion Collider (RHIC), Brookhaven National Laboratory, is investigated for $\sqrt{s_{NN}} = 130$ GeV, the highest center of mass energy yet achieved in collisions between heavy nuclei in the laboratory. The data were collected with the BRAHMS detector during the final 2 weeks of the first RHIC run in August and September 2000, where the beam luminosity reached 10-15% of the nominal design value. We present measurements of the $N(\bar{p})/N(p)$ ratio at rapidities around $y \approx 0, 0.7$ and 2 as a function of collision centrality and transverse momentum together with similar $N(\pi^-)/N(\pi^+)$ ratios at $y \approx 0, 1$ and 3. The beam rapidity is 4.95. The measurements provide the first particle ratios over an extended rapidity range at RHIC energies. It is found that while the meson ratios are close to unity, the measured antiproton to proton ratios decrease from about 62% at $y \approx 0$, to 59% at $y \approx 0.7$ and 44% at $y = 2$ for 0-40% collision centrality. The results show that a net-baryon free midrapidity region has not been attained, although the $N(\bar{p})/N(p)$ ratio is the highest that has been measured so far in nucleus-nucleus collisions. Recently, the STAR collaboration has measured similar particle ratios at $y \approx 0$ in a narrower momentum range [4] and their results agree well with the $y \approx 0$ measurements presented here.

The BRAHMS detector system [5] used in the present measurements consists of two independent magnetic spectrometers that can be positioned over an angular range from 2.3° to 30° (forward spectrometer, FS) and from 30° to 90° (midrapidity spectrometer, MRS) with respect to the beam line. A scintillator tile multiplicity array (TMA) measure charged particle emission in the central pseudorapidity region ($-2.0 < \eta < +2.0$) and is used for centrality selection. This detector consists of 38 square tiles of plastic scintillators ($12 \times 12 \times 0.5$ cm^3). The tiles are grouped in rows of 8 to form a tube of hexagonal cross section with the axis along the beampipe. Panels in the MRS and FS acceptances were not installed in order to minimize secondary interactions. Two detector systems cover forward angles. The Zero Degree Calorimeters (ZDC) [6] at ± 18 m measure non-interacting neutrons from the collisions. The Beam-Beam Counters (BB) consist of two arrays with a total of 70 phototubes, each with a Cerenkov radiator, positioned $\pm$ 2.3 m from the nominal intersection point and measure charged hadrons in the pseudo-rapidity range of $3.0 < |\eta| < 3.8$. These two systems are used to define collision events by two simultaneous measurements of the interaction vertex position.

The collision centrality was determined using the TMA. For each actual vertex position (and corresponding pseudorapidity), the total energy deposited in each ring of TMA tiles is accumulated. The energy loss signal is transformed to charged particle multiplicity via division with the expected average energy deposited by one charged particle in a tile. Centrality cuts are applied by selecting appropriate ranges in the multiplicity spectrum. The cuts can be expressed in terms of the fraction of the nuclear reaction cross section by normalization to the integral of the TMA spectrum obtained with a near minimum bias trigger. This trigger requires energy deposition in each of the two Zero Degree Calorimeters (ZDC) above 25 GeV with the additional condition of at least one tile having a hit. This requirement selects events corresponding to $\approx 97\%$ of the nuclear interaction cross section. Three centrality bins were used in the analysis (0 to 10%, from 10 to 20% and from 20 to 40% of the nuclear interaction cross section).

In the present measurements the MRS was operated at both 90° and 40° and the FS at 4°. The magnets of the two spectrometers were operated at fields allowing the reconstruction of particle tracks with momenta above ≈ 0.2 GeV/c in the MRS and above ≈ 2 GeV/c in the FS. The solid angles subtended by the MRS and FS are 6.0 msr and 0.5 msr, respectively. Both spectrometers consist of two Time Projection Chambers (TPC's) positioned on either side of a Dipole magnet and followed by a segmented scintillator time of flight (TOF) wall for particle identification (PID). In the case of the FS this tracking and PID arrangement is preceded by an additional dipole magnet.

Particle momenta are determined by projecting the straight line tracks as reconstructed in the two TPC's to the magnets and calculating the bending angle of matched tracks using an effective edge field approximation. The momentum resolution is $\delta p/p \approx 0.01 \cdot p$, and $\approx 0.03 \cdot p$ for the FS, and MRS , respectively. Selected MRS tracks are required to originate from the primary vertex as determined by the counters within ± 4 cm horizontally and ± 2.4cm vertically. Tracks in the FS have a much wider requirement on the horizontal (z) matching, due to the uncertainty associated with projecting tracks back to the beam line. Particle identification requires not only a measurement of the time of flight of particles but also the determination of the flight distance and thus of the collision vertex on an event by event basis. In these initial runs, the collision vertex distribution was approximately of Gaussian shape with $\sigma \approx 70$ cm. The BB counters have an intrinsic time resolution of 65 ps and permit a determination of the position of the collision vertex to a precision of ≈ 2 cm by measuring the difference in arrival time of the first particles in the left and right arrays assuming that these particles travel with the velocity of light. This method is confirmed by determining the vertex by projecting tracks determined in the first TPC of the MRS back to the beam plane. The two TOF arrays are positioned at 4.3 m (MRS) and 8.6 m (FS) from the nominal interaction vertex position, respectively. The overall time resolution was determined to σ(TOF)$\approx$ 120 ps and thus permitted the separation of kaons and protons in the momentum range $p < 2.2$ GeV/c and $p < 4.5$ GeV/c in the MRS and FS, respectively.

In the MRS, kaons and pions could be separated up to $p = 1.5$ GeV/c. In the FS, kaons could not be cleanly separated from pions, although the $N(\pi^-)/N(\pi^+)$ ratio in the range $0.15 < p_t < 0.3$ GeV/c could be determined with only a small kaon contamination. Figure 1 demonstrates the PID achieved in the MRS and FS. The lower two panels show the m^2 spectra obtined for positively charged particles (π^+, K^+, p) and the upper two panels show similar information for for negative particles $(\pi^-, K^-, \bar{p})$. The distributions were calculated from $m^2 = p^2(t^2/L^2 - 1)$, where p, t and L denote the particle momentum, flight time, and flight distance, respectively. The MRS data shown are from the $0.4 < p_t < 2.2$ GeV/c interval, while the FS data correspond to the interval $0.15 < p_t < 0.55$ GeV/cF.

The yield of pions, and protons in the FS is determined from the number of tracks that fulfill various fiducial requirements, primarily, that the determined particle time of flight falls within a 2σ band around the calculated time of flight versus momentum curve for the particle mass under consideration (shaded distributions in figure 1). In the MRS the yields are determined by applying the cuts in the m^2 spectra as displayed in Figure 2 by the solid lines. The number of particles measured at either polarity is normalized to the same number of collision events defined by the BB–ZDC coincidences fulfilling a given centrality cut described above and the ratios calculated. The acceptances for the spectrometers for positively charged particles at one field are equal to the acceptances for negatively charge particles at the opposite polarity. Thus in ratios of numbers of particles, measured at opposite field polarities most systemetic errors cancel out. Losses of antiprotons due to anihilation have also been evaluated by GEANT simulations to be about 3 % in the MRS and 9 % in the FS. It is noted that background from mis-identified tracks and tails from kaons and pions peaks are negligible for the measurements at 90° and 40°. At forward angles the contributions from background tracks increase but are still small. Furthermore, it is similar at both polarities and affects the extracted ratios negligibly ($< 1\%$). In the MRS the background contribution from slow protons arising mainly from the interaction of pions with the Be beampipe (has been evaluated to be less than xxx % / has been subtracted from the proton yield) for the p_t range $> .4$GeV/c. In the FS this contribution neglegible. The main source of systematic uncertainties in the particle ratios quoted stem from the run luminosity normalisations, from background slow background protons, and from corrections to anti-proton absorbtion. The normalisations contribute less than $\pm 5\%$. In addition it is important to consider corrections from weak decays of hyperons (see below).

Figure 2 shows the dependence of the measured $N(\bar{p})/N(p)$ ratios on collision centrality and on particle transverse momentum. Ratios were corrected for antiproton absorbtion as described above. Fig. 2a shows the centrality dependence for data summed over all momentum bins, and Fig. 2b shows the p_t dependence for data summed over all centrality bins. The vertical error bars represent statistical errors only, while the horizontal bars indicate the bin size. It is seen that the centrality dependence of the ratio is small for the three considered rapidities. The $N(\pi^-)/N(\pi^+)$ ratios (not shown) exibit a similar lack of centrality and p_t dependence.

The ratios shown in Figure 2 have not been corrected for protons and antiprotons that originate from weak decays of hyperons (Λ, Σ, etc.) and which fall in the acceptance of the spectrometers and passes fiducial tracking cuts. The correction factors will in general depend on the relative production ratios of hyperons (H) and primary baryons (B) and their antiparticles and on the relative slopes of the respective spectra. We have studied the magnitude of the corrections using various model predictions as input to GEANT simulations. Assuming primary H/B ratios of up to 0.5 we find that the correction to the quoted ratios is less than 10% when the anti-Hyperon to Hyperon ratios at y $\approx$ 0 is between 0.4 and 0.8 and at y$\approx$ 2 between 0.3 and 0.5.

Figure 3 summarizes the rapidity dependence of the measured particle ratios calculated for the $0-40\%$ most central collisions. The upper and lower panel depict the $N(\pi^-)/N(\pi^+)$ and $N(\bar{p})/N(p)$ ratios, respectively, obtained in the momentum range dependent on rapidity as described above. Only statistical uncertainties are shown. It is seen that, while the pion ratio is independent of rapidity and very close to unity, the antiproton to proton ratio drops significantly with increasing rapidity.

The $N(\bar{p})/N(p)$ ratio of 0.62 found here at $y \approx 0$ is considerably higher than the similar ratios measured in Pb+Pb collisions at SPS ($\approx 0.07-0.15$ at $\sqrt{s_{NN}}$=17 GeV) [11, 7] and at AGS ($\approx 2.5 \cdot 10^{-4}$ at $\sqrt{s_{NN}} = 5$ GeV) [8]. It is in fact close to the p+p result ($0.61 \pm .1$) from the ISR at $\sqrt{s_{NN}} = 63$ GeV and $p_t \approx 0.3\mathrm{GeV}/c$, and is below the value obtained by extrapolating the p+p systematics collisions to 130 GeV/c CM energy [9]. It is noted that an isospin correction of the ratio measured in p+p collisions will have the result of lowering the $N(\bar{p})/N(p)$ by $\approx 20\%$. Particular interest is attached to the rapidity dependence of the ratios. The present systematics show that the ratios fall off more rapidly over two units of rapidity than the nucleus-nucleus results at lower $\sqrt{s_{NN}}$, but are very similar to the p+p result at roughly half the CM energy [10].

Finally we compare in fig. 3 the measured ratios to calculations using the HIJING model [12], the FRITIOF 7.02 [13] string model and the UrQMD cascade model [14] using the same cuts on centrality and transverse momentum as those applied in the data analysis. All three models reproduce the observed pion ratios well. The FRITIOF model reproduces the $N(\bar{p})/N(p)$ ratios quite well,while it overpredicts by $\approx 30\%$ the charged particle yield at $\eta \approx 0$ [15]. This is mainly related to a fairly large degree of stopping predicted by the model. On the other hand the HIJING model descibes the overall charge particle yields at $\eta \approx 0$ while fails in describing the anti-proton to proton ratios rapidity dependence. This feature of the model is in turn related to a small stopping of the projectile baryons. The UrQMD model underpredicts it by almost a factor of 2. These models examplifies the present understanding of heavy ion collisions at this new energy regime; none of the models offers a consistent description of the observed features.

In summary, the BRAHMS experiment has measured the ratio of positive and negative pions and protons at central and forward rapidities. We find that the pion ratios are close to unity as would be expected at these energies, where about 4000 charged particles (predominantly pions) are produced per central collision [16]. We find, however, that for central collisions at $\sqrt{s_{NN}} = 130$ GeV the ratio of antiprotons to protons is still significantly below unity at midrapidity and decreases towards forward rapidity. The rapidity dependence serves as an indicator of the balance between baryon number transport to the central region and anti-baryon and baryon pair production. This suggests that there is still a significant contribution from participant baryons over the entire rapidity range and that the full transparency of the Bjorken model has not been reached. Nevertheless, reactions at the present energy evidence the highest antiparticle/particle ratios so far observed in energetic nuclear collisions.

The BRAHMS collaboration wishes to thank the RHIC team for the great efforts that have led to the successful startup of the collider and for the support to the experiment. This work was supported by the Division of Nuclear Physics of the Office of Science of the U.S. Department of Energy under contract with BNL (No.DE-AC02-98-CH10886), Texas A&M (FG03-93-ER40773), yyyyy, the Danish Natural Science Research Council, the Norwegian Natural Science Research Council, the Polish ministry of Research, and the Korean Research Foundation Grant

References

[1] J.D. Bjorken, Phys. Rev. **D27**, 140 (1983).

[2] N. Herrmann, J.P. Wessels and T. Wienold, Annu. Rev. Nucl. Part. Sci. **49**, 581 (1999).

[3] F. Videbæk and O. Hansen, Phys. Rev. **C52**, 2584 (1995).

[4] C. Adler et al., The STAR collaboration, Phys. Rev. Lett. (in print).

[5] D. Beavis et al., The BRAHMS collaboration, 'Conceptional Design Report for BRAHMS', BNL-62018 (/www.rhic.bnl.gov/brahms/WWW/cdr/cdr.html).
I.G. Bearden et al., The BRAHMS collaboration, Nuclear Instruments and Methods, to be published;

[6] C.Adler et al., Nucl. Inst. Meth.(2001) submitted, (/xxx.lanl.gov/nucl-ex/0008005).

[7] F. Sickler et al., The NA49 collaboration, Nucl. Phys. **A661**, 45c (1999) and G. E. Cooper, Ph. D. Thesis.

[8] L. Ahle et al., The E802 collaboration, Phys. Rev. Lett. **81**, 2650 (1998).

[9] K.Guettler et al. Nucl.Phys.**B116**, 77 (1076)

[10] P. Capiluppi et al., Nucl. Phys. **B79**, 189 (1974).

[11] I. G. Bearden et al, NA44 collaboration, J. Phys. G, Nucl. Part **23** (1997) 1865, M. Kaneta Ph. D. Thesis (www. .) and *Particle production in Pb+Pb collisions at CERN-SPS* (in prep).

[12] HIJING with Parton shadowing and Jet quench. X-N. Wang and M. Gyulassy, Phys. Rev. D **44** (1991) 3501.

[13] FRITIOF 7.02. H. Pi, Comp. Phys. Comm. (in preparation, or 92?)

[14] S. A. Bass et al, Prog. Part. Nucl. Phys. **41** (1998) 225 and M. Bleicher et al. J. Phys. G. Nucl. Part **25** (1999) 1859.

[15] B.Back et.al. Phys.ReV.Lett.**85**,3100(2000).

[16] J.J.Gardhoje for the BRAHMS Collaboration, Proceedings of Moriond conference 2001, and BRAHMS collaboration (in preparation).

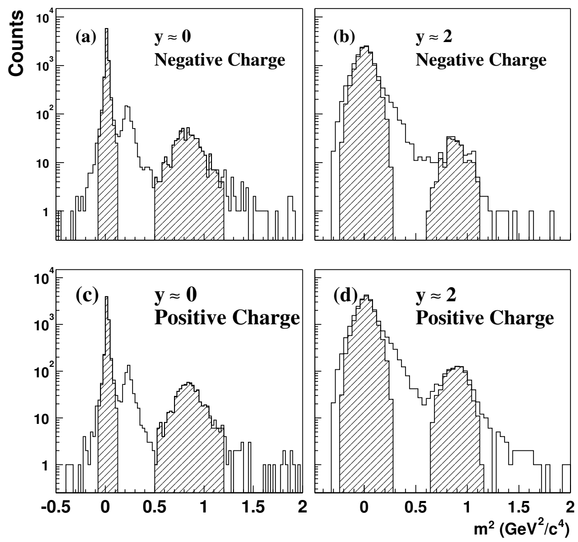

Figure 1: m^2 distributions for charged particles identified in the BRAHMS spectrometers. Left panels (a) and (c) show data for the MRS postioned at 90° with respect to the beam direction, for negatively and positively charged particles, respectively. The hatched area shows the pions selected using momentum independent cuts in m^2 for analysis in the momentum range p < 1.6 GeV/c and $-0.075 < m^2 < 0.125$ and the protons for p ¡2.4 GeV/c and $0.5 < m^2 < 1.2$, in both cases u The right panels (b) and (d) show data from the FS at 4° ($y \approx\ 2$). The hatched region for these panels shows yield of particles selected for analysis on the basis of fiducial cuts on time–of–flight for a momentum range of $2 < p < 4$ GeV/c.

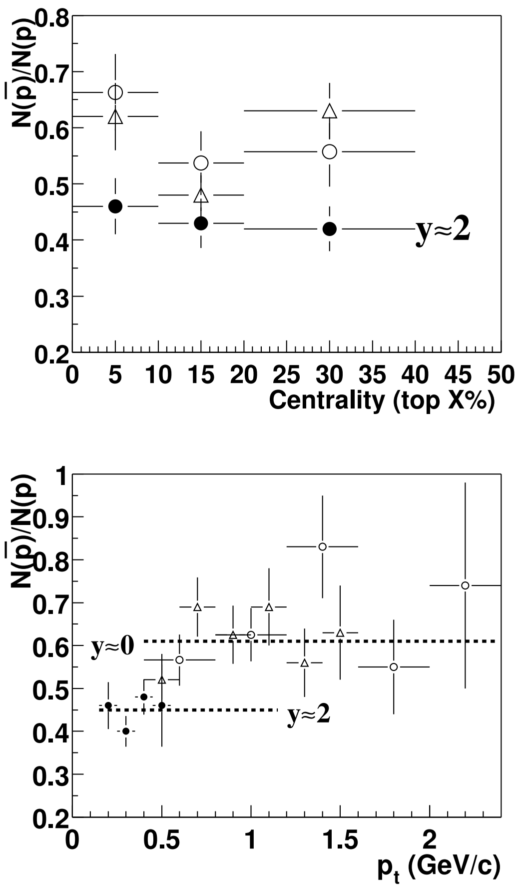

Figure 2: The upper panel shows the centrality dependence of the $N(\bar{p})/N(p)$ ratios for the three rapidity values ($y \approx 0$, $y \approx 0.7$ and $y \approx 2$). The centrality is quoted as the fraction of the geometrical nuclear reaction cross section. The lower panel shows the transverse momentum dependence of the measured $N(\bar{p})/N(p)$ ratio for the three rapidity intervals, for events selected from the $0-40\%$ centrality cut.

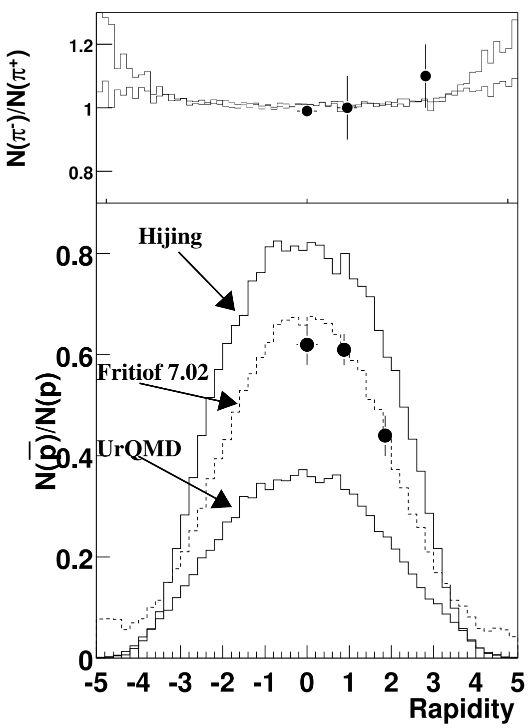

Figure 3: Comparison of the measured $N(\bar{p})/N(p)$ (lower panel) and $N(\pi^-)/N(\pi^+)$ (upper panel) ratios to model predictions. The data shown are for $0 - 40\%$ central events and integrated over the transverse momentum range shown in figure 2. The three calculations using the HIJING model, FRITIOF and UrQMD models discussed in the text are shown.